

Homology modelling and Structural analysis of FLOWERING LOCUS T protein from *Solanum tuberosum*

Ritu Singh¹, Shashi Rawat^{1*}, Vinay Sharma², Jagesh K Tiwari¹ and B. P Singh¹

¹ICAR- Central Potato Research Institute, Shimla - 171 001, Himachal Pradesh, India.

²Department of Bioscience and Biotechnology, Banasthali University, Rajasthan 304022, India.

*Corresponding author: Shashi Rawat; email: shashi29@yahoo.com

Received: 05 February 2016

Accepted: 29 February 2016

Online: 21 March 2016

ABSTRACT

Flowering locus is a key integrator whose induction leads to activation of flowering in plants. The flowering hormone florigen is a universal protein found in flowering plants. In *S. tuberosum* FLOWERING LOCUS T acts as both 'florigen' and 'tuberigen' which initiates flowering and triggers tuber formation respectively. We have determined the homology model of FLOWERING LOCUS T from *S. tuberosum*. This structure confirms the StFT is a subset of phosphatidylethanolamine-binding proteins (PEBP) family as predicted from sequence homology. The model of StFT protein share a similar topology dominated by a large central β -sheet like PEBP's. The homology model of StFT was verified for their stereochemical quality and accuracy. The 3D structure was validated using Structure Validation Server in which 99.3% of residues present in the favoured regions of the Ramachandran Plot. A better understanding of the 3D structure of StFT is helpful in understanding the mechanisms underlying flowering in *S. tuberosum* and in designing mutagenesis strategy to understanding the possible manipulation for future improvement in potato.

Keywords: phosphatidylethanolamine-binding protein; flowering locus; modelling; three dimensional; homology modeling.

1. INTRODUCTION

The flowering time is an important process in the plant life cycle regulated by several genetic pathways including photoperiod, light quality, vernalization, growth and temperature [1]. The principal factors responsible with the photoperiodic induction of flowering are CONSTANS (CO) and FLOWERING LOCUS (FT). The CO encodes a zinc-finger transcription factor whose ectopic expression leads to early flowering in short day length [2]. FT acts as a floral promoter mainly in the photoperiod pathway downstream of CONSTANS. The FT is a floral integrator gene responsible for controlling and/or triggering flowering in plant and acts an important contributor to agricultural productivity and yield. Flowering locus T is a small protein (20-23 kDa) which is located in the photoperiod-dependent pathway [3]. FT is a mobile

flowering signal called 'florigen' which moves freely from leaf through the vasculature to the shoot apical meristem (SAM) to initiate floral evocation and also regulates various developmental changes in plants [4, 5]. FT has a highly conserved sequence and function across angiosperms and acts as a central player in regulating the transition from the vegetative to reproductive phase in plants.

At the shoot apex, the FT protein interacts with FLOWERING LOCUS D (FD) through the basic leucine zipper (bZIP) transcription factor. The FT-FD complex activates the meristem identity gene APETALA1 (MADS-box protein) which stimulate flower development [6]. The function of FT protein as a transport floral signal or floral activators has been identified in dicotyledonous plants such as tomato

Single Flower Truss (SFT) [7], Populus (PtFT1) [8], apple [9], sugar beet (*BvFT2*) [10], cucurbits [11], sunflower [12], pea (*GIGAS*) [13], soybean [14], wheat (*TaFT*) [15] and potato [16] as well as in monocotyledonous plants such rice *Heading-date3a* (*Hd3a*) and *Rice Flowering Locus T1* (*RFT1*) [17], barley (*HvFT*) [15], maize [18] and ornamental plants such as *Ipomoea nil* [19], *Chenopodium rubrum* (CrFTL1, CrFTL2) [20], *Oncidium luridum* [21].

FLOWERING LOCUS T is a member of the CETS protein family which is composed of CENTRORADIALIS (CEN), TERMINAL FLOWER 1 (TFL1) and FT. The FT shares homology with PEBP (phosphatidylethanolamine-binding protein) or RAF kinase inhibitor proteins (RKIPs) which are highly conserved from bacteria to humans [17]. Flowering locus genes are induced by exposure to long days (*A. thaliana*, barley and peas) and also in response to short days (rice, potato and Japanese morning glory). The FT gene overexpression in transgenic plants shows early flowering in both short-day and long-day conditions for instance, transgenic plants overexpressing *Hd3a*, *PtFT1*, *SFT* and *CiFT* genes isolated from rice, poplar, tomato and citrus respectively promote early flowering [22].

The regulation of flowering or induction of early flowering in plants is of great importance in agriculture which leads to the identification of new varieties and accelerates breeding time by shortening seed production time. Therefore, FT is an attractive target for altering flowering time in various agronomically important crops [23, 24]. In tomato and tobacco plants, overexpressing tomato FT homologous gene induces extremely early flowering in both day-neutral species. However in *Allium cepa* different FT genes (AcFT1) regulate flowering and bulb formation in transgenic onions [25].

Solanum tuberosum is a member of the Solanaceae (nightshade) family and is the third most significant noncereal food crop after rice and wheat (<http://faostat.fao.org>). The potato is a short-day plant where tuberization is strongly influenced by daylength, with short days (SD) for promoting tuber formation. Recently it has been shown that FT not only acts as the flowering signal 'florigen' which initiates flowering in potatoes but also acts as 'tuberigen' which triggers tuber formation [16]. This shows that the signaling process for both flowering and tuberization have a common theme. In Andean varieties of potato (*S. tuberosum andigena*) tuberization is induced under short days and cool temperatures [26]. However it has been shown that the ectopic expression of the *Hd3a* gene (*FT* orthologue in rice) or the *StSP6A* (*FT*-paralog in potato) in Andigena plants induces short-day potato to flower and tuberize in long days conditions [27].

Despite, of the great economic importance of potato, our knowledge about the molecular mechanisms of flowering is still limited. So the present study was performed with the aim to understand the 3D-structure

of the *S. tuberosum* FLOWERING LOCUS T (StFT) by computational approach whose structure has not been reported yet. Further to check the reliability and validation of the model, various tools and molecular dynamics method were used to study three dimensional structure of the modeled StFT, which could broaden our understanding for the future improvement in potato production.

2. MATERIALS AND METHODS

Molecular modelling and computations in this study were carried out on Z800 workstation on windows 7 platform by using automated homology modeling program Modeller9.11 (<http://salilab.org>). Validity of 3D structure of modeled protein was further evaluated by PROCHECK (<http://nihserver.mbi.ucla.edu/SAVES>), PROSA (<https://prosa.services.came.sbg.ac.at/prosa.php>) and Verify-3D [28]. Interactive visualization and analysis of molecular structures was carried out in Pymol (<http://pymol.sourceforge.net>). Physical and chemical parameters for protein were calculated by ProtParam (<http://www.expasy.ch/tools/protparam.html>). The complete amino acid sequence of the target protein *S. tuberosum* FLOWERING LOCUS T (StFT) was retrieved from the Uniprot protein database (Accession No M1BBV6; PGSC0003DMG400016180 gene) consisting of 174 amino acid length. The physico-chemical characterization of StFT protein were computed using the Expasy's ProtParam server (<http://web.expasy.org/protparam/>) which computes theoretical isoelectric point (pI), molecular weight, total number of positive and negative residues, extinction coefficient, instability index, aliphatic index and grand average hydropathy (GRAVY).

The three-dimensional protein model of StFT was built by homology modeling approach based on high-resolution crystal structures of homologous proteins. The NCBI Basic Local Alignment Search Tool (BLAST) [29] (<http://ncbi.nlm.nih.gov/Blast>) server was used to retrieve the template structure of the closest homologues available in Brookhaven Protein Data Bank (PDB). Further step consisted of performing multiple alignment of the selected templates and the target sequence using the program ClustalW2 (<http://www.ebi.ac.uk/tools/clustalw2>) [30] with the Blossum 62 substitution matrix with gap penalties of gap start 1 and gap extension 0.1. Further homology modeling of StFT was performed by automated homology modeling program Modeller9.11 [31] using two templates downloaded from the Brookhaven PDB. Models were constructed by comparative modeling using the method of satisfaction of spatial restraints as implemented in the program Modeller. The structurally conserved regions (SCR's) in template protein were identified and query was subsequently aligned to template structure with the align2D command in Modeller9.11. Subsequently, the alignment was manually checked for any mismatch. Using a standard modeling procedure, ten models were generated with Modeller9.11 for StFT

The quality of the models was assessed by Modeller itself (based on the value of the objective function calculated by Modeller). Although the models proved to be of nearly equally good quality. Further the stereochemistry of the models obtained from Modeller9.11 was performed by inspection of the Psi/Phi Ramachandran plot using PROCHECK program accessible at SAVES Server (<http://nihserver.mbi.ucla.edu/SAVES>). The PROCHECK program provides information about the stereochemical quality of a given protein structure and was used to generate Ramachandran plot. All final models were inspected for the DOPE (discrete optimized potential energy) score of modeller output per residues of the model. DOPE score calculated by Modeller program is the distance dependent statistical potential based on probabilistic theory. Further the quality of the fold was inspected with PROSA [32] that allowed all residues in negative energy regions very similar to the template protein and indicates the possible correctness of the model structures. The ProSA-Web-server (<https://prosa.services.came.sbg.ac.at/prosa.php>) was used to test the local and overall quality of the final model to check for energy criteria in comparison with the potential of mean force derived from a large set of known protein structures. We used ERRAT (<http://nihserver.mbi.ucla.edu/ERRATv2>) [33] and VERIFY-3D [28] for other evaluations. Further the solvent accessibility of the amino acid residues in the modelled protein was determined by using ASA-view

(<http://gibk26.bse.kyutech.ac.jp/~shandar/netasa/asa-view/>) [34].

3. RESULTS AND DISCUSSION

The physicochemical properties deduced ProtParam shows that the StFT protein sequence has high percentage of valine (V) and arginine (R) 10.9%, 10.3% respectively and the least was for tryptophan (0.6 %). The total number of positively charged residues (+R) (Arg+Lys) was 20 and the total number of negatively charged residues (-R) (Asp+Glu) was also 20. The aliphatic index (AI) which is defined as the relative volume of a protein occupied by aliphatic side chains (A, V, I and L) is regarded as a positive factor for the increase of thermal stability of globular proteins. The thermostability of the protein is assessed by the aliphatic index. The aliphatic index of StFT protein sequence ranged from 43.21. The stability of a protein is calculated via the instability index which indicates the extent of stability of the proteins. However it is reported that proteins having instability index of less than 40 is stable while more than 40 is unstable. The instability index values of StFT protein sequences were found to be 43.21. The Grand Average hydropathy (GRAVY) value for a protein is calculated as the sum of hydropathy values of all the amino acids, divided by the number of residues in the sequence. The GRAVY indicates the solubility of proteins. A GRAVY index of StFT is -0.376. A negative GRAVY value for StFT describes its hydrophilic nature. The results were shown in table 1.

Table 1: Various physicochemical properties of StFT protein sequence computed by ProtParam.

Name	Source	M. wt	Theoretical pI	-R	+R	Instability index	Aliphatic index	GRAVY
M1BBV6	<i>S. tuberosum</i>	20010.7	6.90	20	20	43.21	85.00	-0.376

Table 2: Selected template for the modelling along with the PDB code and resolution, showing percentage identity with StFT.

Name	Chain	Source	Identity with StFT	Similarity with StFT	with PDB code	Resolution
FT	A	<i>A. thaliana</i>	62.4%	76.4%	1WKP	2.60 Å
Florigen Hd3a	A	<i>O. sativa</i>	61.0%	76.3%	3AXY	2.50 Å

The sequence of flowering locus T protein from *S. tuberosum* PGSC0003DMG400016180 gene was obtained from the Uniprot protein database (Accession No. M1BBV6). The complete sequence of the query was downloaded in FASTA format. The first progress toward constructing the homology model of StFT was a template search, carried out in NCBI-BLAST using Blossum 62 substitution matrix with e-value cut-off of 10. The program provided the most promising template structures for homology modelling. Two crystal structures with high percentage identity and resolution were selected as template for alignment (Table 2) which included crystal structure of Flowering Locus T (Ft) from *A. thaliana* (1WKP) and rice Florigen Hd3a (3AXY) as protein templates. The selected templates (1WKP and 3AXY) were aligned pairwise (globally) to the query sequence StFT using needle

program in EMBOSS-GUI (<http://bips.ustrasbg.fr/EMBOSS>). The identity and similarity between the target and template protein 1WKP was 62.4% and 76.4% respectively and template protein 3AXY showed 61.0% and 76.3% identity and similarity respectively. A multiple sequence alignment was carried out with the StFT and the two selected templates by using multiple sequence algorithm ClustalW (Fig. 1). The structurally conserved regions and structurally variable regions were defined and model was built using Modeller9.11. The program deduces the distance and angle constraints from a template structure and combines them with energy terms for adequate stereochemistry in an objective function that is later optimised in Cartesian space with conjugate gradients and molecular dynamic methods. Ten sets of models were generated. The first model has

lowest DOPE score so this model was selected for further study. The quality of the model was further assessed using Ramachandran plot in PROCHECK validation package. In this model, 90.9% of the amino acid residues were in the favorable regions of the plot for the whole protein, whereas 8.4% of the residues were in the additionally allowed region and 0.7% in generously allowed region and no residue in disallowed region. Altogether 99.3% of the residues were in favored and allowed regions. The phi and psi distributions of the Ramachandran plot of non-Glycine, non-Proline residues and main chain parameters plots for the model are summarized in Ramachandran plot summary (Fig 2). Most of the bond angles, bond length, and torsion angles were between values expected for naturally folded protein. Further refinement of the final StFT model was done by energy minimization of the selected outlier residues using protein report tool. The final and refined 3D structure of the StFT superimposes well on the crystal structure of the templates taken for model building. These results imply that the stereochemical properties and quality of modelled structures are quite consistent. The alpha-trace of StFT generated was found to be similar to resolved crystal structure of

the 1WKP and 3AXY in the same orientation (Fig 3). Further evaluated for recognition of error of the StFT model was done with ProSA-Web-server. ProSA uses knowledge-based potentials of mean force to evaluate model accuracy. ProSA-Web-server analysis revealed that the modelled structure occupies a region of NMR predicted native protein structures of same size with Z score of -5.18. This indicates that the StFT model was sufficiently accurate for the structure based analysis (Fig 4). The VERIFY-3D analysis revealed that 99.39% of the residues has an average 3D-1D score >0.2 showing that the model protein has good over all quality. The ASAVIEW analysis of the solvent accessibility for the model protein reveals that that the accessible residues were present on the outermost ring of the spiral. The solvent accessibility plot of the StFT protein is shown in fig 5. The majority of negatively charged residues (shown as red D, E) positive charged residues (shown as blue R, K, H) and polar uncharged residues (shown in green G, N, Y, Q, S, T, W) were present on the outermost surface and hydrophobic residues (shown as grey) were confined to the inner rings of the spiral. The yellow colour shows the cysteine residues.

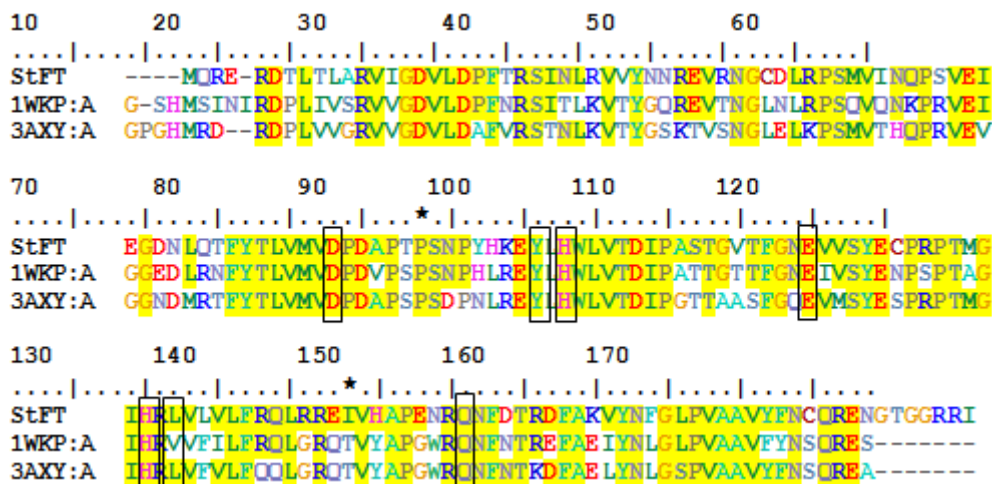


Figure 1: Multiple-sequence alignment of *S. tuberosum* FLOWERING LOCUS T with templates crystal structure of Flowering Locus T (Ft) From *A. thaliana* (1WKP) and Rice Florigen Hd3a (3AXY). Yellow colour indicates the highly conserved regions and black coloured box indicates the conserved motif. The dash represent gaps inserted to maximize the extent of homology among sequences. Asterisks indicate amino acids that are critical to the definition of proteins in the FT. The alignment was produced with BioEdit.

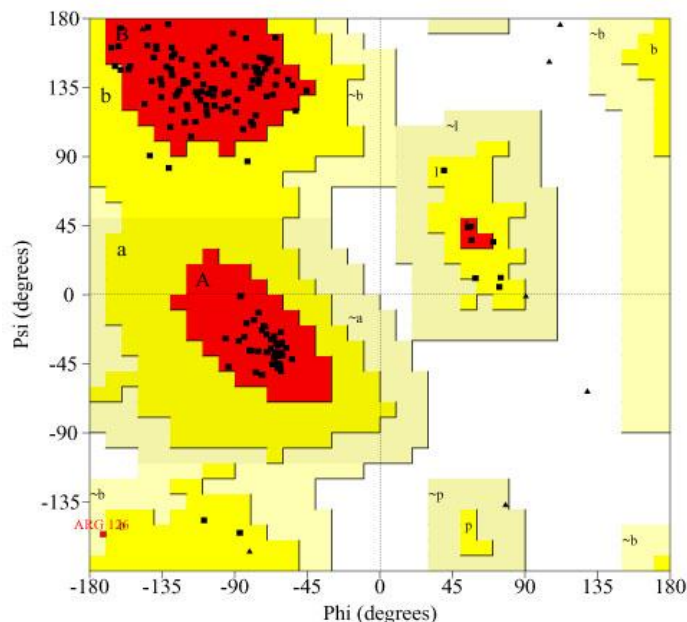
Structural features of StFT and identification of anionic ligand-binding site

Flowering locus T protein from *S. tuberosum* share similar sequence and protein-folding structure to mammalian phosphatidylethanolamine binding protein (PEBP) or Raf1 kinase inhibitor protein (RKIP) [35]. PEBP is a highly conserved group of multifunctional proteins found in bacteria, yeast, nematodes, plants, drosophila and mammals. These proteins play important role in various functions including lipid binding, regulators of several signalling pathways (MAP kinase pathway, NF-kappaB), serine protease inhibition and integrator of flowering process. The PEBP gene family in angiosperms has three subfamilies FLOWERING LOCUS T (FT), MOTHER OF FT AND TFL1

(MFT) and TERMINAL FLOWER1 (TFL1). Like CEN, FT and TFL1 the Flowering locus T from the *S. tuberosum* is a members of a small gene family which encode a phosphatidylethanolamine binding protein that may be a component of membrane complexes involved in signal transduction [36, 37]. In StFT protein the basic protein PEBP protein ranges from 26-163 amino acids in length. The final models include residues 5-167 of the FT sequence from *S. tuberosum*. The StFT PEBP has a large globular fold comprising of five anti parallel central β -sheets (β 3 (62-68), β 4 (82-88), β 5 (99-103), β 6 (115-123) and β 7 (154-161) flanked on one side by subsidiary smaller β -sheets (β 1 (25-28) and β 2 (50-53)) and on the other by two α -helixes α 3 (99-98) and α 4 (141-148) (Fig 6 and 7). The N terminal has a $\alpha\beta$

($\alpha 1$ (5-9) $\beta 1$ $\alpha 2$ (24-46) element present at one terminal. The large central fundamental β -sheet topology has high level of structural homology shared by all structures of PEBP family [38]. The StFT model was compared with the structures of CEN gene of *Antirrhinum majus* which revealed that it contribute to the conformation of the putative anionic ligand-binding site. These include a D-P-D-x-P motif which runs from

residue 68 to 71, a histidine residue at position 84, and a G-x-H-R motif between residues 113 and 116 with possible functional importance. The StFT has a highly conserved potential anion-binding pocket present with high affinity for anions have been observed close to the protein surface. The amino acids residues forming this cavity are conserved among all PEBP family members and constitute the PEB motif.



Ramachandran plot summary

Residues in most favoured regions	130	90.9%
Residues in additional allowed regions	12	8.4%
Residues in generously allowed regions	1	0.7%
Residues in disallowed regions	0	0.0%

Number of non-glycine and nonproline residues	143	100%
Number of end-residues (excl. Gly and Pro)	2	
Number of glycine residues (shown as triangles)	7	
Number of proline residues	12	

Total number of residues **164**

Figure 2: PROCHECK-Ramchandran plot and summary for the homology model of StFT.

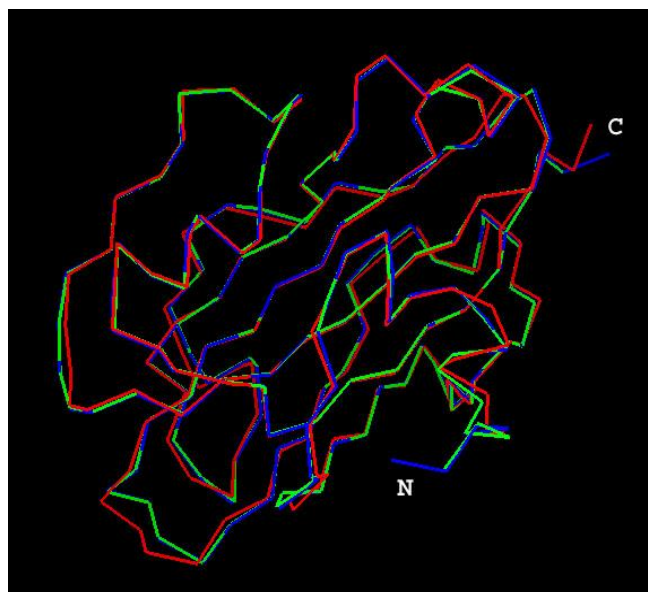


Figure 3: Superposition of alpha-trace of StFT (green), 1WKP (red) and 2AXY (blue). Figure was prepared with PyMol.

helix in StFT as compared to 1WKP and 3AXY. The homology model of StFT has seven β sheet where as two extra small β sheet are seen in the structure of 1WKP and 3AXY which forms loop in homology model

of StFT. Notably another difference is that the StFT and 3AXY has Leu117 and Leu121 where as *A. thaliana* (FT) has Val at position 120 which creates a larger volume of anion binding site.

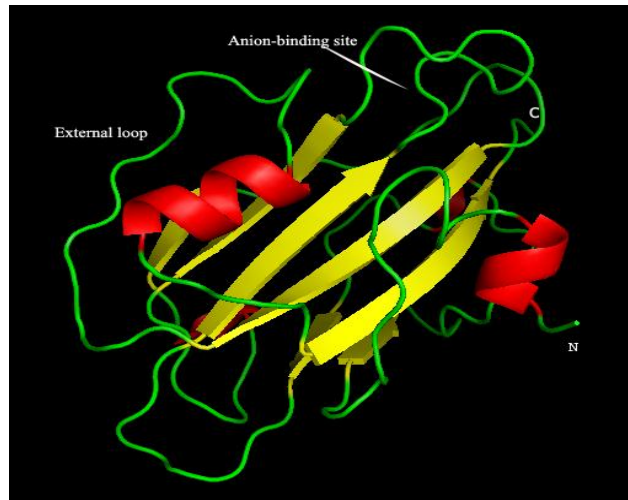


Figure 6: Overall topology of the theoretical structure of StFT showing anion binding site and external loop along with the N-terminal and C-terminal of the protein. The figure was prepared with pymol.

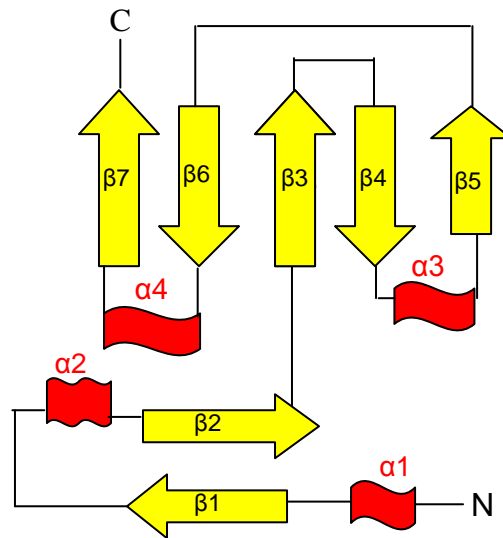


Figure 7: Systematic representation of secondary structure of StFT showing central five antiparallel β sheets ($\beta 3$, $\beta 4$, $\beta 5$, $\beta 6$ and $\beta 7$), four helices ($\alpha 1$, $\alpha 2$, $\alpha 3$, $\alpha 4$) along with the N-terminal and C-terminal of the protein.

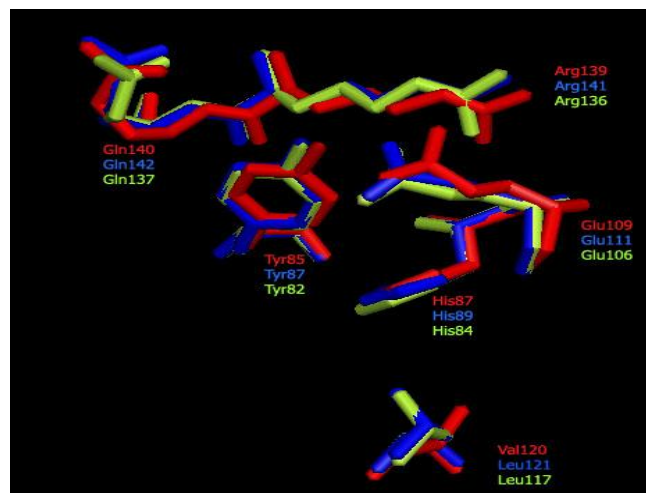


Figure 8: Predicted structure of StFT constructed by homology modelling. The conserved residues for the 1WKP, 3AXY and StFT are shown in red, blue and green respectively.

4. CONCLUSION

In this study we built a high quality homology model of the StFT which shares the highest homology to the *A. thaliana* (FT) and *O. sativa* (Florigen Hd3a). Structural features of StFT protein have been well-characterized by three dimensional modelling. Three-dimensional structure analysis of FLOWERING LOCUS protein from *S. tuberosum* helps to determine its biological functions. The anion binding site shows high conservation similar to most of the PEBP's. Thus modelling effort provides a platform for a systematic mutagenesis strategy. Therefore, understanding the possible manipulation of flowering genes is of great relevance and an interesting target for the future improvement in potato production.

5. Acknowledgements

The authors are grateful to the Director, Central Potato Research Institute, Shimla, for providing the necessary facilities, constant support and encouragement throughout the study.

6. REFERENCES

- Mouradov A, Cremer F and Coupland G (2002). Control of flowering time: interacting pathways as a basis for diversity. *Plant Cell*. 14: 111-130
- Putterill J, Robson F, Lee K, Simon R and Coupland G (1995) The CONSTANS gene of Arabidopsis promotes flowering and encodes a protein showing similarities to zinc finger transcription factors. *Cell*. 80: 847-857
- Kardailsky I, Shukla VK, Ahn JH, Dagenais N, Christensen SK et al (1999). Activation tagging of the floral inducer FT. *Science*. 286: 1962-5
- Kobayashi Y, Kaya H, Goto K, Iwabuchi M and Araki T (1999). A pair of related genes with antagonistic roles in mediating flowering signals. *Science*. 286: 1960-62
- Imaizumi T and Kay SA (2008). Photoperiodic control of flowering: not only by coincidence, *Trends Plant Sci*. 11: 550-558
- Abe M, Kobayashi Y, Yamamoto S, Daimon Y, Yamaguchi A, Ikeda Y, Ichinoki H, Notaguchi M, Goto K and Araki T (2005). FD, a bZIP protein mediating signals from the floral pathway integrator FT at the shoot apex. *Science*. 309: 1052-1056
- Lifschitz E, Eviatar T, Rozman A, Shalit A, Goldshmidt A et al (2006). The tomato FT ortholog triggers systemic signals that regulate growth and flowering and substitute for diverse environmental stimuli. *Proc Natl Acad Sci USA*. 103: 6398-6403
- Hsu CY, Liu YX, Luthe DS and Yuceer C (2006). Poplar FT2 shortens the juvenile phase and promotes seasonal flowering. *Plant Cell*. 18: 1846-1861
- Kotoda N, Hayashi H, Suzuki, M, Igarashi M, Hatsuyama Y et al (2010). Molecular characterization of Flowering Locus T-Like genes of apple (*Malus domestica* Borkh.). *Plant Cell Physiol*. 51: 561-575
- Pin PA, Benlloch R, Bonnet D, Wremerth-Weich E, Kraft T et al (2010). An antagonistic pair of FT homologs mediates the control of flowering time in sugar beet. *Science*. 330: 1397-1400.
- Lin MK, Belanger H, Lee YJ, Varkonyi-Gasic E, Taoka KI et al (2007). FLOWERING LOCUS T protein may act as the long-distance florigenic signal in the cucurbits. *Plant Cell*. 19: 1488-1506
- Blackman BK, Strasburg JL, Raduski AR, Michaels SD and Rieseberg LH (2010). The role of recently derived FT paralogs in sunflower domestication. *Curr Biol*. 20: 629-635
- Hecht V, Laurie RE, Vander Schoor JK, Ridge S, Knowles CL et al (2011). The pea GIGAS gene is a FLOWERING LOCUS T homolog necessary for graft-transmissible specification of flowering but not for responsiveness to photoperiod. *Plant Cell*. 23: 147.
- Kim MY, Shin JH, Kang YJ, Shim SR and Lee SH (2012). Divergence of flowering genes in soybean. *J Biosci*. 37: 857-870.
- Yan L, Fu D, Li C, Blechl A, Tranquilli G et al (2006). The wheat and barley vernalization gene VRN3 is an orthologue of FT. *Proc Natl Acad Sci USA*. 103: 19581-19586
- Navarro C, Abelenda J A, Cruz-Oro E, Cuellar CA, Tamaki S et al (2011). Control of flowering and storage organ formation in potato by FLOWERING LOCUS T. *Nature*. 478: 119-122
- Kojima S, Takahashi Y, Kobayashi Y, Monna L, Sasaki T, Araki T and Yano M (2002). Hd3a, a Rice ortholog of the Arabidopsis FT gene, promotes transition to flowering downstream of Hd1 under short-day conditions. *Plant Cell Physiol*. 43: 1096-1105
- Meng X, Muszynski MG and Danilevskaia ON (2011). The FT-Like ZCN8 gene functions as a Floral Activator and is involved in photoperiod sensitivity in Maize. *Plant Cell*. 23: 942-960
- Hayama R, Agashe B, Luley E, King R and Coupland G (2007) A circadian rhythm set by dusk determines the expression of FT homologs and the short-day photoperiodic flowering response in *Pharbitis*. *Plant Cell*. 19: 2988-3000
- Cháb D, Kolar J, Olson MS and Storchova H (2008). Two Flowering Locus T (FT) homologs in *Chenopodium rubrum* differ in expression patterns. *Planta*. 228: 929-940
- Hou CJ and Yang CH (2009). Functional analysis of FT and TFL1 orthologs from orchid (*Oncidium goweri* ramsey) that regulate the vegetative to reproductive transition. *Plant Cell Physiol*. 50: 1544-1557
- Lee J and Lee I (2010). Regulation and function of SOC1, a flowering pathway integrator. *J Exp Bot*. 61: 2247-2254
- Kobayashi Y and Weigel D (2007). Move on up, it's time for change-mobile signals controlling photoperiodic-dependent flowering. *Genes Dev*. 21: 2371-2384
- Turck F, Formara F and Coupland G (2008). Regulation and identity of florigen: FLOWERING LOCUS T moves centre stage. *Annu. Rev. Plant Biol*. 59: 573-594
- Lee R, Baldwin S, Kenel F, McCallum J and Macknight R (2013). FLOWERING LOCUS T genes control onion bulb formation and flowering. *Nat Commun*. 4: 2884
- Ewing EE and Struik PC (1992). Tuber formation in potato: Induction, initiation, and growth. *Hortic Rev*. 14: 89-198
- Jackson SD (1999). Multiple signalling pathways control tuber induction in potato. *Plant Physiol*. 119: 1-8.
- Eisenberg D, Luthy R and Bowie JU (1997) VERIFY3D: assessment of protein models with three-dimensional profiles. *Methods Enzymol*. 277: 396-404
- Altschul SF, Gish W, Miller W, Myers EW and Lipman DJ (1990) Basic local alignment search tool. (1990). *J Mol Biol*. 215: 403-10
- Larkin MA, Blackshields G, Brown NP, Chenna R, McGettigan PA et al (2007). Clustal W and Clustal X version 2.0. *Bioinformatics*. 23: 2947-8
- Sali A and Blundell TL (2009). Comparative protein modelling by satisfaction of spatial restraints. *J Mol Biol*. 234: 283-291
- Wiederstein M and Sippl MJ (2007). ProSA-web: interactive web service for the recognition of errors in three-dimensional structures of proteins. *Nucleic Acids Res*. 35: 407-410
- Colovos C and Yeates TO (1993). Verification of protein structures: patterns of nonbonded atomic interactions. *Protein Sci*. 2: 1511-1519
- Ahmad S, Gromiha M, Fawareh H and Akinori S (2004). ASAview: database and tools for solvent accessibility representation in proteins. *BMC Bioinform*. 5: 51
- Schoentgen F and Jollès P (1995). Review From structure to function: possible biological roles of a new widespread protein family binding hydrophobic ligands and displaying a nucleotide binding site. *FEBS Lett*. 369: 22-26
- Bradley D, Carpenter R, Copsey L, Vincent C, Rothstein S and Coen E (1996). Control of inflorescence architecture in *Antirrhinum*. *Nature*. 379: 791-7
- Bradley D, Ratcliffe O, Vincent C, Carpenter R and Coen E (1997). Inflorescence commitment and architecture in *Arabidopsis*. *Science*. 275: 80-83

38. Banfield MJ and Brady RL (2000). The structure of Antirrhinum Centroradialis protein (CEN) suggests a role as a kinase regulator. *Mol Biol Evol*. 297: 1159-1170
39. Ahn JH, Miller D, Winter VJ, Banfield MJ, Lee JH, Yoo SY, Henz SR, Brady RL and Weigel D (2006). A divergent external loop confers antagonistic activity on floral regulators FT and TFL1. *EMBO J*. 25: 605-614
40. Hanzawa Y, Money T and Bradley D (2005). A single amino acid converts a repressor to an activator of flowering. *Proc Natl Acad Sci USA*. 21: 7748-7753.

© 2016; AIZEON Publishers; All Rights Reserved

This is an Open Access article distributed under the terms of the Creative Commons Attribution License which permits unrestricted use, distribution, and reproduction in any medium, provided the original work is properly cited.
